communications earth & environment

Article

https://doi.org/10.1038/s43247-024-01860-3

Light-dependent methane production by a coccolithophorid may counteract its photosynthetic contribution to carbon dioxide sequestration

Yuming Rao [1], Guang Gao [1,2], Ilana Berman-Frank[3], Mina Bizic [4,5] & Kunshan Gao [1,2]

Many phytoplankton produce methane, a potent greenhouse gas. However, little is known about the relationship between their methane production and photosynthesis, which drives carbon sequestration in the oceans. Here, by ruling out the possibility of classical methanogenesis, we show that the bloom-forming marine microalga *Emiliania huxleyi* released methane during photosynthesis (did not generate it in darkness) while grown under different light levels, the amount of methane released correlated positively with photosynthetic electron transfer and carbon fixation. Under growth-saturating light, *E. huxleyi* produces methane at a maximal rate of about 6.6 ×10^{-11} μg cell^{-1} d^{-1} or 3.9 μg g^{-1} particulate organic carbon d^{-1}. The microalga released up to 7 moles methane while fixing about 10^5 moles of carbon dioxide. Considering the higher global warming potential of methane than that of carbon dioxide and complicated processes involved in methane air-sea fluxes, the warming potential of phytoplankton methane production should be broadly evaluated.

The methane (CH_4) mixing ratio in the atmosphere has increased from 715 ppbv in the preindustrial era to around 2000 ppbv at present[1]. CH_4 traps more heat per molecule than carbon dioxide (CO_2), yet it has a shorter atmospheric lifetime (half-lifetime ca. 10 years), making its global warming potential ~80-fold more powerful than CO_2 during the first 20 years after it is released, and about 30-fold higher over the course of a century[2]. Thus, CH_4 is the second most important source of anthropogenic greenhouse gas following CO_2. Consequently, understanding the sources and sinks of CH_4 in the marine realm is essential for projecting the magnitude of future global warming and exploring mitigation solutions for the remediation of short-lived greenhouse gases.

Vast amounts of CH_4 are produced in the oceans. Yet, the proportions of CH_4 released from the oceans to the atmosphere have traditionally been considered minor[3,4]. Nevertheless, frequently observed oversaturation of CH_4 in the oxygenated upper mixed layer in both ocean and lake ecosystems[5–11] challenges the previous understanding that CH_4 formation occurs exclusively under anoxic conditions in aquatic environments[12]. Methanogenic archaea living in anoxic micro-environments[13–16] and physical transport of CH_4 from the anoxic sediments may contribute to the CH_4 oversaturation in the upper mixed layer[17,18]. However, such mechanisms are unlikely for pelagic open-water environments due to CH_4 oxidation by CH_4-oxidizing bacteria and the thermocline's physical barrier preventing sediment-derived CH_4 from reaching the surface water[19]. Additionally, classical methanogenic activity is not commonly detected in surface marine waters[20,21].

Prokaryotic[22–24] and eukaryotic phytoplankton[9,10,25–27] have been found to release CH_4, and this CH_4 produced by phytoplankton living in surface waters may escape to the atmosphere before oxidation[3,4]. In three marine microalgae (*Emiliania huxleyi*[26], *Chrysochromulina* sp. and *Phaeocystis globose*[27,28]) and in cyanobacteria[24], the addition of ^{13}C-labeled bicarbonate resulted in the formation of ^{13}C-labeled CH_4. In several marine and freshwater cyanobacteria, both CH_4 production and photosynthetic O_2 evolution ceased when different photosynthetic inhibitors, acting both on PSI and PSII, were added, further confirming that these phytoplankton species release CH_4 during photosynthesis[24]. Isotopic patterns of CH_4 released by phytoplankton are distinguishable from

[1]State Key Laboratory of Marine Environmental Science, College of Ocean and Earth Sciences, Xiamen University, Xiamen, China. [2]Co-Innovation Center of Jiangsu Marine Bio-industry Technology, Jiangsu Ocean University, Lianyungang, 222005, China. [3]Department of Marine Biology, Leon H. Charney School of Marine Sciences, University of Haifa, Haifa, Israel. [4]Department of Environmental Microbiomics, Institute for Technical Environmental Protection, Technical University of Berlin, Berlin, Germany. [5]Department of Plankton and Microbial Ecology, Leibniz Institute of Freshwater Ecology and Inland Fisheries, Zur alten Fischerhütte 2, 16775 Stechlin, Germany. e-mail: ksgao@xmu.edu.cn

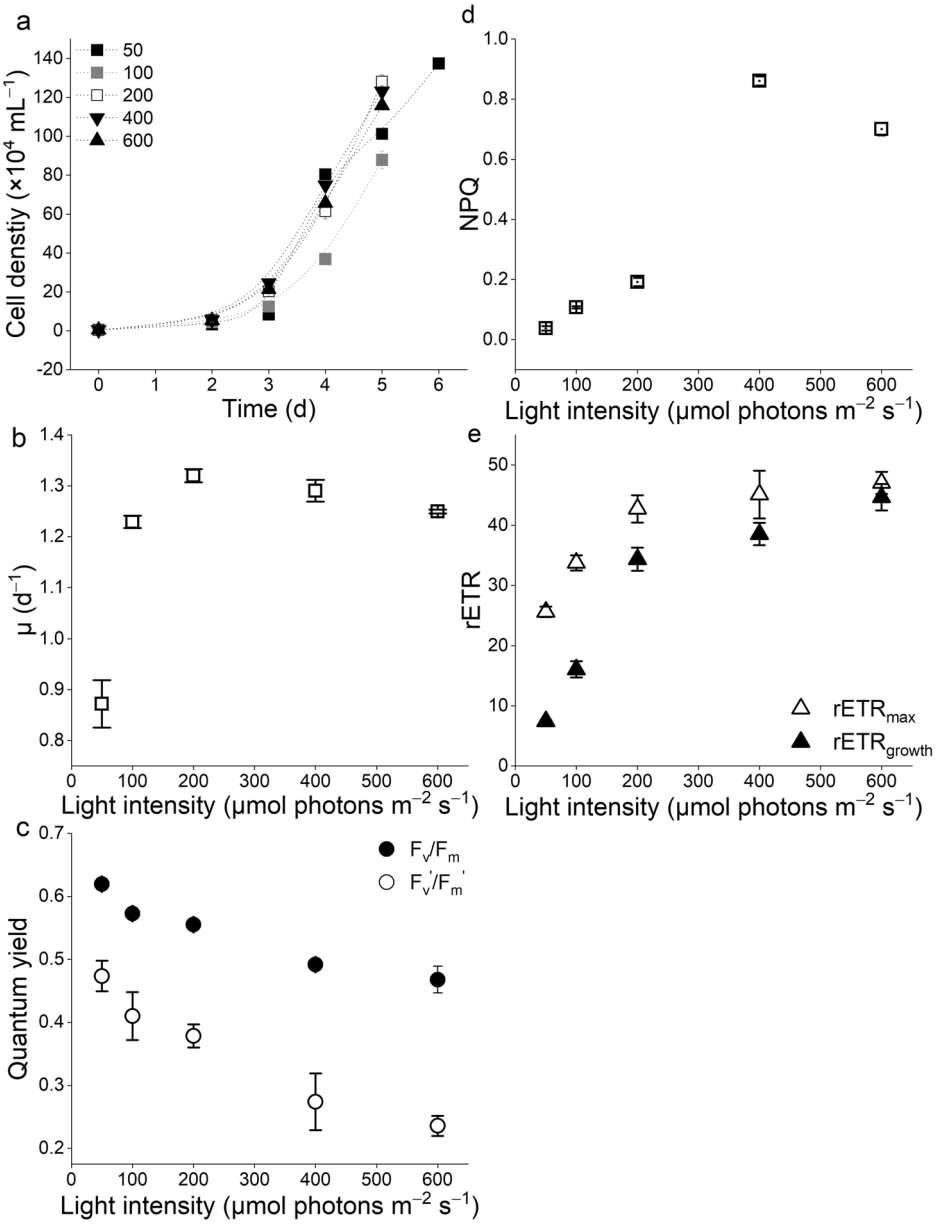

Fig. 1 | Cell growth and photosynthetic parameters of *Emiliania huxleyi* grown under different light intensities. Cell densities of *E. huxleyi* over time when grown under different light intensities (**a**), specific growth rate during the exponential growth phase (**b**), and photochemical parameters of *E. huxleyi* as a function of growth light intensities (**c**–**e**); maximal quantum yield (F_v/F_m) and effective quantum yield (F_v'/F_m') (**c**); non-photochemical quenching (NPQ) (**d**); maximum relative electron transport rate ($rETR_{max}$) and rETR under growth light ($rETR_{growth}$) (**e**). (error bars mark the standard deviation for triplicate cultures).

those formed by methanogenic archaea, indicating a novel yet unknown pathway[29,30].

Emiliania huxleyi is an essential contributor to the ocean's primary production[31] and carbon cycles while providing a significant source of dimethyl sulfide (DMS)[32] and releasing CH_4 from photosynthetically fixed CO_2[26,28]. To date, it remains unknown how CH_4 production by *E. huxleyi* correlates with its photosynthetic activity. By examining the relationship between CH_4 production rate and photosynthetic performance in *E. huxleyi*, we found that CH_4 production increases proportionally with photosynthetic electron transfer and carbon fixation under illumination, with no CH_4 release detected in the darkness. Our findings allowed us to establish the CH_4 production quotient (MPQ), expressing the quantity of CH_4 released versus that of CO_2 fixed by photosynthesis. Considering the higher global warming potential of CH_4, this parameter established for different CH_4-generating phytoplankton species may be utilized in estimating the counteractive role of phytoplankton CH_4 production to photosynthetic CO_2 removal via the marine biological CO_2 pump in both laboratory and in situ observations.

Results

Specific growth rate and fluorescence parameters

The growth stages and pattern of *E. huxleyi* were similar for cultures grown at light intensities from 50 to 600 μmol photons m^{-2} s^{-1} with a lag phase for the first 3 days followed by the exponential phase from day 3 through 6 (Fig. 1a). The specific growth rates of *E. huxleyi*, calculated from the exponential growth phase, increased by ~51 % when the light intensity increased from 50 to 200 μmol photons m^{-2} s^{-1}. At higher light intensities, - reaching 400 μmol photons m^{-2} s^{-1}, growth rates were similar ($p = 0.73$). The slight decline in growth measured for cultures at 600 μmol photons m^{-2} s^{-1} was not statistically significant ($p = 0.18$) (Fig. 1b). The effective and maximal quantum yield declined as growth irradiance increased while non-photochemical quenching (NPQ) was enhanced as irradiance increased (Fig. 1c, d). The maximal relative electron transport rates ($rETR_{max}$), derived from the fitted rapid light curves (Supplementary Fig. 2) and from growth light levels ($rETR_{growth}$), increased as growth light intensity increased until being saturated at light levels >200 μmol photons m^{-2} s^{-1} (Fig. 1e).

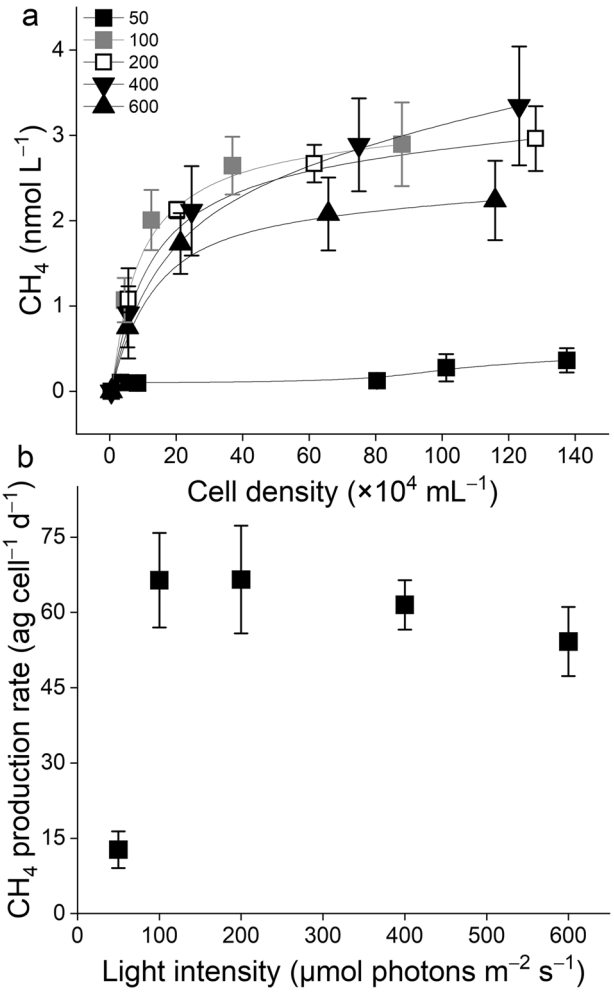

Fig. 2 | CH_4 production in *E. huxleyi* cultures as a function of light. CH_4 concentrations as a function of algal cell densities of *E. huxleyi* (**a**) and CH_4 production rate (**b**) during the exponential phase (Fig. 1a) under different light intensities. Different symbols and numbers (**a**) represent the light levels in μmol photons m^{-2} s^{-1} (error bars mark the standard deviation for triplicate cultures).

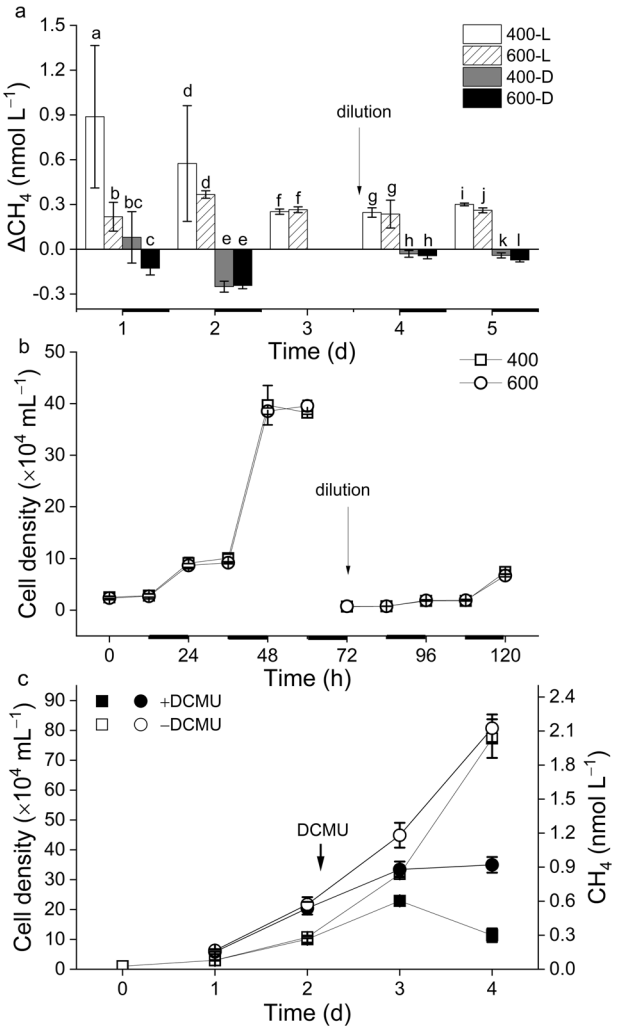

Fig. 3 | Changes in CH_4 concentrations in *E. huxleyi* cultures during the light and dark periods and the effect of photosynthetic inhibitor DCMU on CH_4 production and cell growth. The changes in CH_4 concentrations (ΔCH_4) produced in *E. huxleyi* cultures during 12 h from either the light or dark phase from cultures acclimated to two light intensities (400 and 600 μmol photons m^{-2} s^{-1}) (**a**), parallel cell densities of *E. huxleyi* during the measurement periods (**b**). The changes in cell growth (square symbols) and CH_4 production (circle symbols) (**c**) after the addition of the electron transfer inhibitor DCMU. In panels **a** and **b**, the arrow represents the dilution timings and bolder lines on the x-axis represent dark periods; in panel **c**, the arrow represents the addition of DCMU. 400 and 600 represent the daytime light intensities (μmol photons m^{-2} s^{-1}). L and D represent light and dark periods. Error bars mark the standard deviation for triplicate cultures. The letters above the bars in **a** mark significant differences between the treatments ($p < 0.05$) during the experimental period.

Cell growth and CH_4 production

Accumulation of CH_4 in the cultures increased with elevated cell densities (Fig. 2a). CH_4 production increased by ~423% when light intensities doubled from 50 to 100 μmol photons m^{-2} s^{-1} ($p < 0.05$). The CH_4 production rate (per day) leveled off at light levels >200 μmol photons m^{-2} s^{-1} (Fig. 2b). CH_4 production was detected only during the light period with the increase of algal cell density (Fig. 3a), with CH_4 evolution approaching zero or negative during the dark period, irrespective of algal cell density (Fig. 3b). The addition of photosynthetic inhibitor DCMU in the culture reduced both the microalga growth and its CH_4 production (Fig. 3c)

The CH_4 production rate, carbon fixation rate, and cell size of *E. huxleyi* concurrently increased from the initiation of light and peaked at the end of the light period (Fig. 4a–c). Accordingly, the CH_4 production quotient increased linearly during the light period (Fig. 4d, $R^2 = 0.9708$ and 0.9713 for cells grown under 200 and 100 μmol photons m^{-2} s^{-1}, respectively). Furthermore, *E. huxleyi* production of CH_4 positively correlated with CO_2 fixation and cell size (Supplementary Figs. 4, 5).

Relationship between photosynthetic electron transport and CH_4 production rates

The relationships between POC-specific production rates of CH_4 with growth irradiance and electron transport rate were similar to typical photosynthesis-light curves (Fig. 5). POC content increased linearly with increased light to peak at ~270 μmol photons m^{-2} s^{-1} and then declined at the PAR levels >300 μmol photons m^{-2} s^{-1} (Fig. 5a). When CH_4 production was normalized to POC, saturation was reached at ~440 μmol photons m^{-2} s^{-1} ($p < 0.05$) with no significant decline in production at the higher irradiances (Fig. 5b). The relationship between CH_4 production and photosynthesis could be illuminated by plotting the relative electron transport rates (rETR) with the POC-specific CH_4 production rates yielding a linear and positive correlation ($R^2 = 0.975$, $p < 0.05$, Fig. 5c).

Ensuring methanogenic archaea and bacteria did not contribute to the measured CH_4

To ensure CH_4 was not produced by any heterotrophic methanogens in the culture, *E. huxleyi* cells were grown with the methanogenic inhibitor,

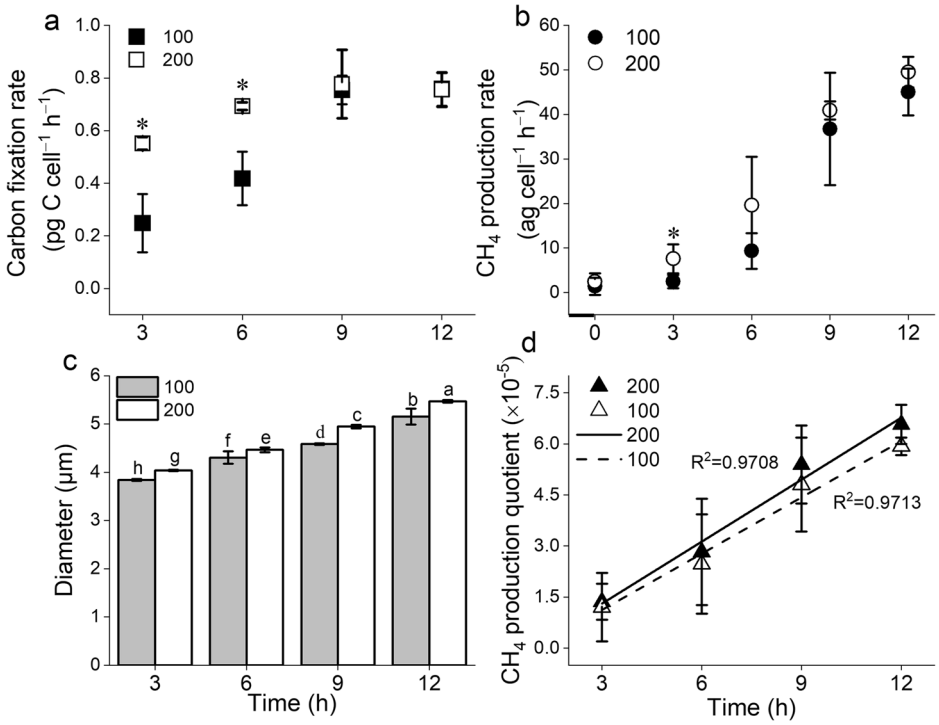

Fig. 4 | Changes in carbon fixation rates, CH_4 production rates, cell size and the estimated CH_4 production quotient as a function of time under light. Changes during the 12 h light period in photosynthetic carbon fixation rates (**a**), CH_4 production rates (**b**), and algal cell diameters (**c**) of *E. huxleyi* cultures as measured every 3 h. Calculated CH_4 production quotients (the ratio of CH_4 released to CO_2 fixed) for cultures grown at 100 and 200 μmol photons m^{-2} s^{-1} (**d**) (error bars mark the standard deviation for triplicate cultures). The asterisks and letters above the bars mark statistically significant ($p < 0.05$) differences between the treatments.

sodium 2-bromoethanesulphonate (2-BES). The addition of the inhibitor did not significantly affect CH_4 production ($p = 0.70$ and $p = 0.41$ under the light levels of 200 or 100 μmol photons m^{-2} s^{-1}, respectively) (Supplementary Fig. 6). Moreover, the algae-free filtrate showed negligible (<3% of the CH_4 produced in algal cultures) production over a period of 3-4 days (Supplementary Fig. 7).

Discussion

In the present study, the CH_4 production by *Emiliania huxleyi* is light-dependent and positively correlated with photosynthetic electron transport and C fixation (Figs. 4, 5). Since we ruled out disturbances from methanogenic archaea and heterotrophic bacteria in the cultures (Supplementary Figs. 6, 7) and found that *E. huxleyi* cultures did not produce CH_4 in the dark (Fig. 3a), it is obvious that the CH_4 produced in the microalgal culture is directly linked to photosynthesis. The established methane production quotient (MPQ: molar CH_4 released vs molar CO_2 fixed) (Fig. 4d) based on the simultaneous measurement of CH_4 production and C fixation indicates that *E. huxleyi* can release up to 7 CH_4 moles while fixing 10^5 moles of CO_2.

Phytoplankton are known to produce the volatile dimethyl sulfide (DMS), an important infochemical mediating microbial interactions[33]. There is a possibility that the CH_4 produced by the microalga is due to the photolysis of DMS[34]. However, it is unlikely in the present study, since the observed CH_4 production was about 1 nmol L^{-1} per day in our culture of the *E. hux* PMLB 92-11 that can produce about 120 nmol L^{-1} DMS per day[33], and only 0.2 nmol L^{-1} daily aerobic production of CH_4 was observed during a DMS-spiking (20 μmol L^{-1}) experiment[34]. Thus, a possible explanation for this photosynthesis-associated CH_4 production is likely a result of the Fenton reaction driven by reactive oxygen species (ROS)[35] with methylated intracellular metabolites serving as substrates. On the other hand, during photosynthesis, NADPH is produced in the light reaction and oxidized in the dark reaction[36]. ROS could be produced during the oxidization of NADPH during the dark reaction[37] and Mehler reaction[38] or simply generated due to the transfer of electrons to oxygen[39] in the light reaction. Therefore, when the light intensity increased above 260 μmol photons m^{-2} s^{-1} (optimal growth light), it is possible that enhanced accumulation of ROS under high light stress[40–42] could promote CH_4 formation[35]. This explains the observed linear correlation of $rETR_{max}$ and POC-normalized CH_4 production rate (Fig. 5c). *E. huxleyi* cells increase their size under illumination (Fig. 4c), indicating accumulation of organic matter during the light period. Thus, methylated metabolites produced via photosynthesis likely serve as an internal substrate, explaining the positive correlation between CH_4 production, C fixation and cell size (Supplementary Figs. 4, 5), the higher POC-normalized CH_4 production rate under high light intensities (Fig. 5b), and the increased CH_4 production quotient during the light period (Fig. 4d). In *E. huxleyi* RCC1216, the POC-normalized CH_4 production rate was not inhibited at high light levels[28]. In contrast, in the subarctic strain used in this study, isolated off the coast of Bergen, Norway (~61 °N), CH_4 production was saturated at 440 μmol photons m^{-2} s^{-1} (Fig. 5b) and somewhat inhibited at higher light intensities (Fig. 2c). It is therefore likely that different *E. huxleyi* strains naturally adapted to different light regimes, display varying differences between CH_4 production and light.

Calcification in *E. huxleyi* has been suggested to act as an electron sink[43] and is known to increase with enhanced light intensities[44]. Strain PMLB 92-11, used in the present work, did not calcify (Supplementary Fig. 3), although previous studies showed it calcifies at a rate lower than other strains (3.6 pg C $cell^{-1}$ d^{-1}[44] for PMLB 92-11 vs 8.96 pg C $cell^{-1}$ d^{-1} for RCC1216[45]). It is not clear whether the calcification process correlates with the CH_4 release in *E. huxleyi*. Nevertheless, the CH_4 production rate in the non-calcifying strain PMLB 92-11 (Fig. 2b) was higher than that of the calcifying strain RCC1216 under similar light levels[28]. As calcification acts as an electron sink[43] and since the POC-normalized CH_4 production rate is highly dependent on photosynthetic electron transfer (Fig. 5c), the calcification in *E. huxleyi* likely down-regulates CH_4 production, which needs to be experimentally tested.

Emiliania huxleyi occurs in oceans worldwide, with the most extensive known temperature range for phytoplankton between 1-31 °C, and it can form blooms in many oceanic regions[31,46]. The light intensities we used in this study fall within the typical daytime mean light intensities during *E. huxleyi* blooms, which range from 200-800 μmol photons m^{-2} s^{-1}[47]. We showed that CH_4 production is light-dependent; therefore, higher light intensities in the field likely result in higher CH_4 production. In addition to light levels, other ongoing environmental changes, including intensive UV radiation, ocean warming, decreasing pH (ocean acidification), and eutrophication may also influence CH_4 production by phytoplankton and

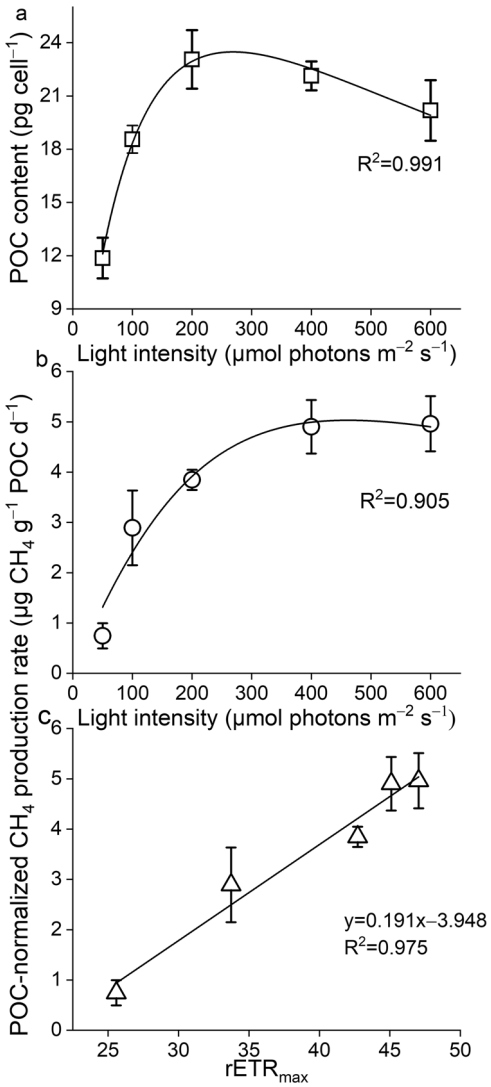

Fig. 5 | The correlation of CH_4 production rate per particulate organic carbon (POC) with light or relative electron transport rate ($rETR_{max}$). The effects of light on the cellular content of POC (**a**) and on POC-normalized CH_4 production rates (**b**) in cultures of *E. huxleyi* grown at different light levels. When the POC-normalized CH_4 production rates were examined in relation to the photophysiological status of the *E. huxleyi* cells a significant linear increase in CH_4 production as a function of $rETR_{max}$ as derived from RLC (see Supplementary Fig. 2) was observed (**c**). ($n = 3$; error bars mark the standard deviation for triplicate cultures).

subsequent upward flux of CH_4 to the atmosphere[48], although little has been documented on these aspects[28,49].

CH_4 produced from autotrophs may, to some extent, offset their contribution via photosynthetic CO_2 fixation to the marine biological carbon pump (BCP). The CO_2 fixed by phytoplankton photosynthesis and associated CH_4 release may alter concentrations of CO_2 and CH_4 in the upper oceans, which may affect their fluxes to the atmosphere (Fig. 6). To the best of our knowledge, this study is the only one so far to quantify CH_4 production quotients (MPQ). Provided that different *E. huxleyi* strains exhibit similar levels of MPQ (Supplementary Table 1), underlying counteractive roles of their CH_4 production against their contributions to carbon sequestration should be evaluated in different waters and/or with different phytoplankton types by taking CH_4 oxidation, different timescales of POC remineralization[50] and RDOC production by phytoplankton[51] into consideration (Fig. 6). The major gaps in understanding the counteractive role and the contribution of phytoplankton-released CH_4 to the upward CH_4 flux from the oceans may lie in interpreting CH_4 generating and oxidizing dynamics in ocean environments[4] and the extent of how much the primary producers including *E. huxleyi* contribute to RDOC accumulation in terms of their carbon fixation.

Phytoplankton species tested so far release CH_4[52], with cyanobacteria producing CH_4 10–100 times higher than eukaryotic phytoplankton[29]. Therefore, the MPQ values can be smaller in microalgae than cyanobacteria since their photosynthetic carbon fixation rates per Chl *a* do not usually change over one order. As progressive ocean warming is suggested to decrease vertical POC transport and to enhance the remineralization of organic matter[53], the counteractive warming potential of phytoplankton-produced CH_4 remains to be further examined. Our methodology and results provide a new perspective to look into the potential importance of phytoplankton-related CH_4 production, and suggest that the coupling of CH_4 production and photosynthetic CO_2 fixation in phytoplankton can affect the capacities of the oceanic sink and source of these greenhouse gases, which are closely related to the feedback of marine ecosystems to climate change (Fig. 6) (Supplementary Table 1). Therefore, investigating how phytoplankton CH_4 production vs CO_2 fixation differ in different regions, especially in waters where phytoplankton blooms are stimulated by global warming[29,54], is expected in future research.

Methods

Monoalgal cultures and experimental setup

Emiliania huxleyi PMLB 92-11 (isolated from Bergen coast, Norway) was cultured in batch or semi-continuous culture mode in artificial seawater (ASW) enriched with Aquil medium with initial nitrogen and phosphorus concentrations of 100 and 10 μmol L^{-1}[55], respectively. In batch cultures, the initial cell density was set at 5000 cells mL^{-1} and reached a final concentration of more than 1× 10^6 cells mL^{-1}, corresponding to the initial and late exponential growth phase. Cells were diluted every two days in the semi-continuous cultures to maintain the exponential growth phase. Cells were acclimated to a day-night cycle of 12 h light and 12 h dark at 20 °C at different light intensities (50–600 μmol photons m^{-2} s^{-1}, measured with a probe of the multi-color PAM) of white-light (ST5-LED10, FLS, China) for >15 generations before experiments on CH_4 release.

After the microalga had acclimated to different light levels (see above), we determined its growth rates, photosynthetic C fixation rates, photochemical parameters (non-photochemical quenching, quantum yield, relative electron transport rate (rETR)), biochemical parameters (total particulate carbon, particulate organic carbon), and CH_4 production. Once the relationship between CH_4 production of the microalga and light had been established, cells grown under 400 and 600 μmol photons m^{-2} s^{-1} (in batch mode without renewing the medium) or at 100 and 200 μmol photons m^{-2} s^{-1} (in semi-continuous mode, with the culture medium renewed every 72 h) were selected to estimate CH_4 production rates and their relationship with photosynthetic C fixation. These light levels were chosen because we could verify the rates of CH_4 production above and below light-saturating conditions.

To investigate algal CH_4 production processes, we designed a closed chamber system using 1.1 L borosilicate bottles filled with 800 mL artificial seawater and 300 mL headspace volume. These bottles were sealed with lids (GL 45, 3 ports) equipped with two three-way ports (one for gas sampling and another for water sampling and an orifice to maintain air pressure during gas sampling, Supplementary Fig. 1). To establish the relationship between CH_4 production and photosynthetic C fixation in *E. huxleyi*, measurements of CH_4 production and photosynthetic C fixation were conducted simultaneously for 3 h during the cells' exponential growth phase.

Measurements of specific growth rate

Samples were collected every 12 or 24 h in batch or semi-continuous cultures. Diurnal variations of cell density and cell diameter were measured every 3 h. Cell density and size were determined using a particle counter and size analyzer (Z2 Coulter, Beckman, U.S.A.). The specific growth rate (μ)

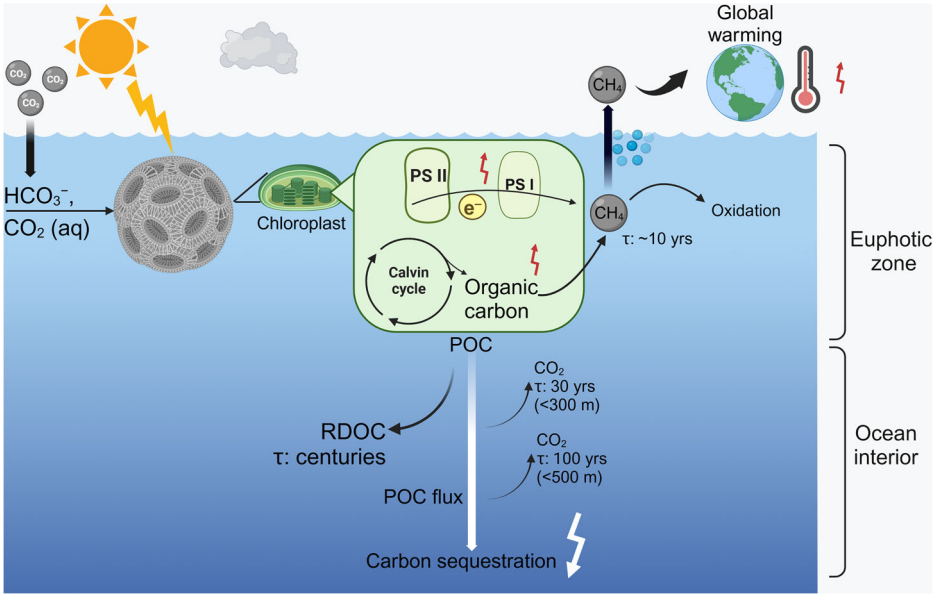

Fig. 6 | Conceptual illustration of CH_4 production by the microalga *Emiliania huxleyi*. The CH_4 produced during photosynthesis and the microalgal carbon sequestration exhibit antagonistic feedbacks to global warming. The photosynthesis-driven CH_4 in the oceans may affect its upward flux, thereby likely counteract phytoplankton carbon sequestration involving refractory dissolved organic carbon (RDOC) and biological CO_2 pump (BCP).

was calculated based on the following formula:

$$\mu\left(d^{-1}\right) = \left(\ln N_1 - \ln N_0\right)/\left(t_1 - t_0\right) \quad (1)$$

where N_1 and N_0 represent the cell concentrations at t_1 and t_0, respectively.

Determination of CH_4 production rate

The CH_4 mixing ratio in the headspace of 1.1 L borosilicate bottles was measured using the Picarro G2308 (Picarro Inc., CA, USA), which is capable of detecting concentrations as low as 1 ppb. The gas flow rate was set at 230 mL min^{-1}. Before sampling, all flasks were gently shaken to equilibrate the gas and water phases. 300 mL of gas samples were removed from each bottle using a syringe and injected into the instrument. The length of the injection is at least 1 min to maintain stable readings during the measurement. The gas sampling procedure was conducted according to Lenhart et al.[26] with some modifications (as written in Zou et al.[56] and shown in Supplementary Fig. 1) as follows: the headspace was replaced with the same volume of sterile air with a known CH_4 mixing ratio; the gas in the headspace (300 mL) was mixed back and forth using the two syringes (one of which containing sterile air and another one is empty) with 300 mL sterile air before measurement, the CH_4 mixing ratio of the sterile air was taken into consideration in subsequent calculations. The CH_4 mixing ratio in the headspace was calculated using the CH_4 mixing ratio of the sterile air and mixed gas sample based on the modified equation[56]:

$$C_{CH_4} = \left(C_M \times 600 - C_{air} \times 300\right)/300 \quad (2)$$

where C_{CH_4} indicates the mixing ratio of CH_4 in the headspace, C_M represents the CH_4 mixing ratio in the mixed gas samples measured, C_{air} denotes the CH_4 mixing ratio of the sterile air.

CH_4 mass in each bottle's headspace was calculated according to the ideal gas law from the CH_4 mixing ratio (ppmv) as follows:

$$m_{CH_4} = \frac{P}{R \times T} \times C_{CH_4} \times V \times M_{CH_4} \quad (3)$$

where P is pressure in atm, T temperature in K, R ideal gas constant in L atm mol^{-1} k^{-1}, V the volume of the headspace in L, C_{CH_4} the mixing ratio of CH_4 in the headspace, M_{CH_4} the molar weight of CH_4. The concentration of CH_4 in the water phase was calculated according to Bunsen solubility coefficient[57] and the formula[58] based on the headspace CH_4 mixing ratio, temperature and salinity of the water phase as follows:

$$CH_4\left(nmol\,L^{-1}\right) = \left(C_{g2} - C_{g1}\right)\cdot\left(\left(\beta/V_m\right)\cdot R\cdot T + V_g/V_l\right) \quad (4)$$

where C_{g2} and C_{g1} represent CH_4 concentration at time t_2 and t_1 in nmol L^{-1}, respectively. β is the Bunsen solubility coefficient of CH_4 in the seawater in L L^{-1} atm^{-1}, V_m is the molar volume of CH_4 in L mol^{-1}, T temperature in K, R ideal gas constant in L atm mol^{-1} k^{-1}, V_g and V_l represent the volume of gas phase and water phase, respectively.

CH_4 production rate was calculated according to Eq. (5)[26]:

$$P_{CH_4} = q_{CH_4} \times \mu \quad (5)$$

where P_{CH_4} is the CH_4 production rate, q_{CH_4} the CH_4 quota in ng CH_4 $cell^{-1}$, which is the quotient of CH_4 concentration divided by corresponding cell density. μ is the specific growth rate.

Determination of chlorophyll *a* fluorescence

The cells of *E. huxleyi* were cultured semi-continuously within a range of $5 \times 10^3 - 1 \times 10^5$ cells mL^{-1} under different light intensities. The maximal quantum yield of PSII (F_v/F_m), the effective quantum yield of PSII (Yield), and rapid light curves (RLCs) were determined using a Multi-color PAM (Walz, Germany) during the exponential growth period. The saturated pulse for F_v/F_m measurement was set at 3500 μmol photons m^{-2} s^{-1} (10 s). F_v/F_m values were obtained after having the cells dark-adapted for 15 min. The effective quantum yields were measured during the light period, with the actinic light levels being the same as those in the growth conditions. The maximum relative electron transport rate ($rETR_{max}$) was obtained based on the rapid light curves by fitting to the equation[59] (Supplementary Fig. 2).

Application of the photosynthetic inhibitor 3- (3,4-Dichlorophenyl)−1,1-dimethylurea

The photosynthetic inhibitor 3- (3,4-Dichlorophenyl)−1,1-dimethylurea (DCMU) was used to inhibit electron transport from PS II to PQ[60] and added in the culture to a final concentration of 10 μM[61]. The initial cell density was 1×10^5 cells mL^{-1} and grown under 200 μmol photons m^{-2} s^{-1} for two days before DCMU was added. Samples were taken every 24 h at the end of the dark period following the sampling procedure described above.

Measurement of photosynthetic carbon fixation

A ~20 mL subsample of each culture was transferred into 25 mL borosilicate bottles, and 100 µL of 5 µCi $NaH^{14}CO_3$ (ICN Radio chemicals, USA) was added prior to the incubation. Triplicate samples of each bottle were prepared, of which two were illuminated by the growth irradiance, and one was wrapped tightly in aluminum foil to serve as a dark control. After 3-hour incubations, the culture subsamples were immediately filtered onto GF/F filters with low vacuum pressure (<0.03 MPa) under dim light as previously described[62]. Filters were fumed with pure HCl overnight to convert all non-assimilated $H^{14}CO_3^-$ into CO_2 and then dried in a constant temperature oven at 60 °C for over 6 h. The amount of $H^{14}CO_3^-$ incorporated by the algae was counted with a liquid scintillation counter (Beckman, LS6500, Germany) in the presence of 5 mL scintillation cocktail (Hisafe 3, Perkin-Elmer, USA). The photosynthetic C fixation rate was determined according to Gao et al. [62].

Cellular C and N analysis

GF/F filters were pre-combusted at 450 °C for 6 h to eliminate the original organic carbon on the filters. Duplicate subsamples were filtered from one bottle for particulate organic carbon and nitrogen and for inorganic carbon (POC, PON, PIC) analyses. The filter used for POC analysis was fumed with HCl for 12 h, while the other filter for total particulate carbon (TPC) analysis was not treated with HCl. Samples were dried at 60 °C overnight prior to the measurement by using a CHNS elemental analyzer (Vario EL cube Elementar, Germany). PIC content was obtained by subtracting POC from TPC.

Exclusion of disturbance from methanogenic archaea and bacteria

To exclude potential CH_4 production by methanogenic archaea or bacteria, we used PC membranes (1.2 µm) to filter off the algal cells immediately after all measurements and then cultured the bacteria-containing filtrate under the same light and temperature for another 3 (400 and 600 µmol photons m^{-2} s^{-1}) or 4 (100 and 200 µmol photons m^{-2} s^{-1}) days to measure any heterotrophically produced CH_4. The gas sampling procedure was the same as described above. In parallel, we supplemented the cultures with 2-bromoethanesulfonic acid (2-BES) (final concentration of 5 mM), which is a known inhibitor of the key co-enzyme Methyl co-enzyme M reductase of methanogenic archaea[63]. 2-BES was added to the culture, and gas samples from the headspace were taken every 3 h during the light period (Supplementary Fig. 1).

Data analyses

The results were expressed as mean values ± standard deviation ($n = 3$) for three independent replicate cultures. The statistical significance of the data was analyzed with one-way ANOVA or two-way ANOVA (Fig. 4) and the Tukey test at a significance level of $p<0.05$.

Data availability

The source data that supports the findings of this study are available from the Dryad (http://datadryad.org/stash/share/ebQ6YWmDonVkBlmoAgaxY6v5ogiJ8qoBoGyRcsChSNA).

Received: 15 April 2024; Accepted: 30 October 2024;
Published online: 12 November 2024

References

1. Lan, X., Thoning, K. W. & Dlugokencky, E. J. *Trends in globally-averaged CH_4, N_2O, and SF_6 determined from NOAA Global Monitoring Laboratory measurements* (NOAA, 2024).
2. IPCC. *Climate Change 2013: The physical science basis. Contribution of working group I to the fifth assessment report of the Intergovernmental Panel on Climate Change* (Cambridge Univ Press, 2013).
3. Weber, T., Wiseman, N. A. & Kock, A. Global ocean methane emissions dominated by shallow coastal waters. *Nat. Commun.* **10**, 4584 (2019).
4. Resplandy, L. et al. A synthesis of global coastal ocean greenhouse gas fluxes. *Glob. Biogeochem. Cy* **38**, e2023GB007803 (2024).
5. Scranton, M. I. & Brewer, P. G. Occurrence of methane in the near-surface waters of the western subtropical North-Atlantic. *Deep-Sea Res Pt I* **24**, 127–138 (1977).
6. Damm, E. et al. Methane production in aerobic oligotrophic surface water in the central Arctic Ocean. *Biogeosciences* **7**, 1099–1108 (2010).
7. Donis, D. et al. Full-scale evaluation of methane production under oxic conditions in a mesotrophic lake. *Nat. Commun.* **8**, 1661 (2017).
8. Günthel, M. et al. Contribution of oxic methane production to surface methane emission in lakes and its global importance. *Nat. Commun.* **10**, 5497 (2019).
9. Günthel, M. et al. Photosynthesis-driven methane production in oxic lake water as an important contributor to methane emission. *Limnol. Oceanogr.* **65**, 2853–2865 (2020).
10. Hartmann, J. F. et al. High spatiotemporal dynamics of methane production and emission in oxic surface water. *Environ. Sci. Technol.* **54**, 1451–1463 (2020).
11. Thottathil, S. D., Reis, P. C. & Prairie, Y. T. Magnitude and drivers of oxic methane production in small temperate lakes. *Environ. Sci. Technol.* **56**, 11041–11050 (2022).
12. Ferry, J. G. & Lessner, D. J. Methanogenesis in marine sediments. *Ann. NY Acad. Sci.* **1125**, 147–157 (2008).
13. de Angelis, M. A. & Lee, C. Methane production during zooplankton grazing on marine phytoplankton. *Limnol. Oceanogr.* **39**, 1298–1308 (1994).
14. Grossart, H.-P., Frindte, K., Dziallas, C., Eckert, W. & Tang, K. W. Microbial methane production in oxygenated water column of an oligotrophic lake. *Proc. Natl Acad. Sci.* **108**, 19657–19661 (2011).
15. Bogard, M. J. et al. Oxic water column methanogenesis as a major component of aquatic CH_4 fluxes. *Nat. Commun.* **5**, 5350 (2014).
16. Damm, E., Thoms, S., Beszczynska-Möller, A., Nöthig, E.-M. & Kattner, G. Methane excess production in oxygen-rich polar water and a model of cellular conditions for this paradox. *Polar Sci.* **9**, 327–334 (2015).
17. Encinas Fernández, J., Peeters, F. & Hofmann, H. On the methane paradox: Transport from shallow water zones rather than in situ methanogenesis is the major source of CH_4 in the open surface water of lakes. *J. Geophys. Res. Biogeosci.* **121**, 2717–2726 (2016).
18. Peeters, F., Encinas Fernandez, J. & Hofmann, H. Sediment fluxes rather than oxic methanogenesis explain diffusive CH_4 emissions from lakes and reservoirs. *Sci. Rep.-Uk* **9**, 243 (2019).
19. Tang, K. W., McGinnis, D. F., Ionescu, D. & Grossart, H.-P. Methane production in oxic lake waters potentially increases aquatic methane flux to air. *Environ. Sci. Tech. Let.* **3**, 227–233 (2016).
20. Repeta, D. J. et al. Marine methane paradox explained by bacterial degradation of dissolved organic matter. *Nat. Geosci.* **9**, 884–887 (2016).
21. Wäge, J., Schmale, O. & Labrenz, M. Quantification of methanogenic Archaea within Baltic Sea copepod faecal pellets. *Mar. Biol.* **167**, 1–7 (2020).
22. Beversdorf, L., White, A., Björkman, K., Letelier, R. & Karl, D. Phosphonate metabolism by *Trichodesmium* IMS101 and the production of greenhouse gases. *Limnol. Oceanogr.* **55**, 1768–1778 (2010).
23. Teikari, J. E. et al. Strains of the toxic and bloom-forming *Nodularia spumigena* (cyanobacteria) can degrade methylphosphonate and release methane. *ISME J.* **12**, 1619–1630 (2018).
24. Bižić, M. et al. Aquatic and terrestrial cyanobacteria produce methane. *Sci. Adv.* **6**, eaax5343 (2020).

25. Scranton, M. I. & Farrington, J. W. Methane production in the waters off Walvis Bay. *J. Geophys Res.* **82**, 4947–4953 (1977).
26. Lenhart, K. et al. Evidence for methane production by the marine algae *Emiliania huxleyi*. *Biogeosciences* **13**, 3163–3174 (2016).
27. Klintzsch, T. et al. Methane production by three widespread marine phytoplankton species: release rates, precursor compounds, and potential relevance for the environment. *Biogeosciences* **16**, 4129–4144 (2019).
28. Klintzsch, T. et al. Effects of temperature and light on methane production of widespread marine phytoplankton. *J. Geophys. Res. Biogeosci* **125**, e2020JG005793 (2020).
29. Bižić, M. Phytoplankton photosynthesis: an unexplored source of biogenic methane emission from oxic environments. *J. Plankton Res.* **43**, 822–830 (2021).
30. Klintzsch, T. et al. Stable carbon isotope signature of methane released from phytoplankton. *Geophys. Res. Lett.* **50**, e2023GL103317 (2023).
31. Hopkins, J., Henson, S. A., Painter, S. C., Tyrrell, T. & Poulton, A. J. Phenological characteristics of global coccolithophore blooms. *Glob. Biogeochem. Cy* **29**, 239–253 (2015).
32. Holligan, P. M. et al. A biogeochemical study of the coccolithophore, *Emiliania huxleyi*, in the North Atlantic. *Glob. Biogeochem. Cy* **7**, 879–900 (1993).
33. Archer, S. D., Ragni, M., Webster, R., Airs, R. L. & Geider, R. J. Dimethyl sulfoniopropionate and dimethyl sulfide production in response to photoinhibition in *Emiliania huxleyi*. *Limnol. Oceanogr.* **55**, 1579–1589 (2010).
34. Zhang, Y. & Xie, H. Photomineralization and photomethanification of dissolved organic matter in Saguenay River surface water. *Biogeosciences* **12**, 6823–6836 (2015).
35. Ernst, L. et al. Methane formation driven by reactive oxygen species across all living organisms. *Nature* **603**, 482–487 (2022).
36. Beer S., Björk M., Beardall J. *Photosynthesis in the marine environment* (John Wiley & Sons, 2014).
37. Li, Y., Xu, S.-S., Gao, J., Pan, S. & Wang, G.-X. Chlorella induces stomatal closure via NADPH oxidase-dependent ROS production and its effects on instantaneous water use efficiency in *Vicia faba*. *Plos One* **9**, e93290 (2014).
38. Kozuleva, M. Recent advances in the understanding of superoxide anion radical formation in the photosynthetic electron transport chain. *Acta Physiol. Plant* **44**, 92 (2022).
39. Magnani, F. & Mattevi, A. Structure and mechanisms of ROS generation by NADPH oxidases. *Curr. Opin. Struc Biol.* **59**, 91–97 (2019).
40. Pospíšil, P. Production of reactive oxygen species by photosystem II as a response to light and temperature stress. *Front Plant Sci.* **7**, 1950 (2016).
41. Waring, J., Klenell, M., Bechtold, U., Underwood, G. J. & Baker, N. R. Light-induced responses of oxygen photoreduction, reactive oxygen species production and scavenging in two diatom species 1. *J. Phycol.* **46**, 1206–1217 (2010).
42. Plummer, S., Taylor, A. E., Harvey, E. L., Hansel, C. M., & Diaz, J. M. Dynamic regulation of extracellular superoxide production by the coccolithophore *Emiliania huxleyi* (CCMP 374). *Front. Microbiol.* **10**, 1546 (2019).
43. Xu, K. & Gao, K. Reduced calcification decreases photoprotective capability in the coccolithophorid *Emiliania huxleyi*. *Plant Cell Physiol.* **53**, 1267–1274 (2012).
44. Zhang, Y. & Gao, K. Photosynthesis and calcification of the coccolithophore *Emiliania huxleyi* are more sensitive to changed levels of light and CO_2 under nutrient limitation. *J. Photoch. Photobio. B* **217**, 112145 (2021).
45. Rokitta, S. D. & Rost, B. Effects of CO_2 and their modulation by light in the life-cycle stages of the coccolithophore *Emiliania huxleyi*. *Limnol. Oceanogr.* **57**, 607–618 (2012).
46. McIntyre, A., Bé, A. W. & Roche, M. B. Modern Pacific Coccolithophorida: a paleontological thermometer. *Transac NY Acad. Sci.* **32**, 720–731 (1970).
47. Nanninga, H. & Tyrrell, T. Importance of light for the formation of algal blooms by *Emiliania huxleyi*. *Mar. Ecol. Prog. Ser.* **136**, 195–203 (1996).
48. Rees, A. P. et al. Nitrous oxide and methane in a changing Arctic Ocean. *Ambio* **51**, 398–410 (2022).
49. McLeod, A., Brand, T., Campbell, C., Davidson, K. & Hatton, A. Ultraviolet radiation drives emission of climate-relevant gases from marine phytoplankton. *J. Geophys. Res. Biogeosci.* **126**, e2021JG006345 (2021).
50. Wang, W. et al. Transit time distributions and apparent oxygen utilization rates in northern South China Sea using chlorofluorocarbons and sulfur hexafluoride data. *J. Geophys. Res. Oceans* **126**, e2021JC017535 (2021).
51. Jiao, N. et al. Microbial production of recalcitrant dissolved organic matter: long-term carbon storage in the global ocean. *Nat. Rev. Microbiol.* **8**, 593–599 (2010).
52. Liu, L.-Y. et al. Microbial methane emissions from the non-methanogenesis processes: A critical review. *Sci. Total Environ.* **806**, 151362 (2022).
53. Wohlers, J. et al. Changes in biogenic carbon flow in response to sea surface warming. *Proc. Natl Acad. Sci.* **106**, 7067–7072 (2009).
54. Visser, P. M. et al. How rising CO_2 and global warming may stimulate harmful cyanobacterial blooms. *Harmful algae* **54**, 145–159 (2016).
55. Morel, F. M., Rueter, J., Anderson, D. M. & Guillard, R. Aquil: a chemical defined phytoplankton culture medium for trace metal studies. *J. Phycol.* **15**, 135–141 (1979).
56. Zou, C. et al. Correlation of methane production with physiological traits in *Trichodesmium* IMS 101 grown with methylphosphonate at different temperatures. *Front. Microbiol.* **15**, 1396369 (2024).
57. Wiesenberg, D. A. & Guinasso, N. L. Equilibrium Solubilities of Methane, Carbon Monoxide, and Hydrogen in Water and Sea Water. *J. Chem. Eng. Data* **24**, 356–360 (1979).
58. Johnson, K. M., Hughes, J. E., Donaghay, P. L. & Sieburth, J. M. Bottle-calibration static head space method for the determination of methane dissolved in seawater. *Anal. Chem.* **62**, 2408–2412 (1990).
59. Ralph, P. J. & Gademann, R. Rapid light curves: a powerful tool to assess photosynthetic activity. *Aquat. Bot.* **82**, 222–237 (2005).
60. Fuerst, E. P. & Norman, M. A. Interactions of herbicides with photosynthetic electron transport. *Weed Sci.* **39**, 458–464 (1991).
61. Wang, C., Baseler, S. & Lin, S. Glycerol Utilization By Phytoplankton1. *J. Phycol.* **56**, 1157–1167 (2020).
62. Gao, K. et al. Solar UV radiation drives CO_2 fixation in marine phytoplankton: a double-edged sword. *Plant Physiol.* **144**, 54–59 (2007).
63. Logroño, W., Nikolausz, M., Harms, H. & Kleinsteuber, S. Physiological effects of 2-bromoethanesulfonate on hydrogenotrophic pure and mixed cultures. *Microorganisms* **10**, 355 (2022).

Acknowledgements

This study was supported by National Natural Science Foundation of China (No. 42361144840) to K.G. and the joint NSFC-Israel Science Foundation (ISF) grant No. 3051/23 to I.B.F. The authors thank the laboratory engineers Xianglan Zeng and Wenyan Zhao for their logistical and technical support. M.B. was supported by DFG project BI 1987/2-1. The *Emiliania huxleyi* strain PMLB 92-11, originally isolated from the field station of the University of Bergen, Norway, was obtained from the GEOMAR Helmholtz Center for Ocean Research, Kiel, Germany.

Author contributions

K.S.G. and Y.M.R. contributed to design, plan the experiment and write the paper. Y.M.R. performed the experiments. G.G., M.B. and I.B.-F. contributed to analysis of the data and writing of the paper. All of the authors contributed data analysis, revisions, and editing.

Competing interests

The authors declare no competing interests.

Additional information

Supplementary information The online version contains supplementary material available at https://doi.org/10.1038/s43247-024-01860-3.

Correspondence and requests for materials should be addressed to Kunshan Gao.

Peer review information *Communications Earth & Environment* thanks the anonymous reviewers for their contribution to the peer review of this work. Primary Handling Editor: Alice Drinkwater. A peer review file is available.